

Novel Robust High Dynamic Range Image Watermarking Algorithm Against Tone Mapping

Yongqiang Bai¹, Gangyi Jiang^{1,2}, Hao Jiang¹, Mei Yu^{1,2}, Fen Chen¹ and Zhongjie Zhu³

¹ Faculty of Information Science and Engineering, Ningbo University, Ningbo, China

² National Key Lab of Software New Technology, Nanjing University, Nanjing, China

³ Ningbo Key Lab. of DSP, Zhejiang Wanli University, Ningbo, China

[e-mail: jianggangyi@126.com, yumei2@126.com]

*Corresponding author: Gangyi Jiang, Mei Yu

*Received March 21, 2017; revised September 20, 2017; revised January 29, 2018; accepted April 6, 2018;
published September 30, 2018*

Abstract

High dynamic range (HDR) images are becoming pervasive due to capturing or rendering of a wider range of luminance, but their special display equipment is difficult to be popularized because of high cost and technological problem. Thus, HDR images must be adapted to the conventional display devices by applying tone mapping (TM) operation, which puts forward higher requirements for intellectual property protection of HDR images. As the robustness presents regional diversity in the low dynamic range (LDR) watermarked image after TM, which is different from the traditional watermarking technologies, a concept of watermarking activity is defined and used to distinguish the essential distinction of watermarking between LDR image and HDR image in this paper. Then, a novel robust HDR image watermarking algorithm is proposed against TM operations. Firstly, based on the hybrid processing of redundant discrete wavelet transform and singular value decomposition, the watermark is embedded by modifying the structure information of the HDR image. Distinguished from LDR image watermarking, the high embedding strength can cause more obvious distortion in the high brightness regions of HDR image than the low brightness regions. Thus, a perceptual brightness mask with low complexity is designed to improve the imperceptibility further. Experimental results show that the proposed algorithm is robust to the existing TM operations, with taking into account the imperceptibility and embedded capacity, which is superior to the current state-of-art HDR image watermarking algorithms.

Keywords: High dynamic range image, watermarking, watermarking activity, tone mapping, perceptual brightness mask

This work was supported by the Natural Science Foundation of China under Grant nos. U1301257, 61671258 and 61671412, the National High-tech R&D Program of China under Grant no. 2015AA015901, the Natural Science Foundation of Zhejiang Province under Grant no. LY15F010005. It is also sponsored by K.C. Wong Magna Fund in Ningbo University.

1. Introduction

High dynamic range (HDR) contents have recently received significant recognition in many multimedia applications, such as digital photography, ultra-high-definition movies and television, video games, medical imaging, and so on [1-3]. Unlike traditional low dynamic range (LDR) images, HDR images provide a large range of luminance, and they could more accurately represent real scenes and provide rich color details and light levels as they are perceived by human eye [4]. Unfortunately, due to the high cost and technical problems, the special display equipment for HDR image is quite few. Thus, the use of tone mapping operators (TMOs) is necessary when HDR images have to be displayed on traditional displays, so as to generate adaptive LDR data retaining as much information as possible from the original HDR objects while reducing the overall contrast [5]. As digital image itself is easy to be copied, spread and tampered, the issue of intellectual property protection for HDR image also needs to be solved. Although the digital watermarking of LDR image is quite mature, the existing technologies cannot be directly transplanted into HDR image because of the storage formats of HDR images and the variability of TMOs [6]. Therefore, it is necessary for HDR image to develop efficient watermarking algorithms against traditional attacks and TMOs.

Currently, HDR image watermarking researches have been paid more and more attentions. Yu et al. [7], Wang et al. [8] and Chang et al. [9,10] directly exploited HDR image's RGBE format storage features to embed lossless watermark. Based on the least significant bit (LSB) approach, Cheng et al. [11] and Li et al. [12] embedded the watermark in the HDR image's RGBE and LogLuv (TIFF) formats, respectively. Lin et al. [13] proposed a watermarking scheme, based on the fact that the mantissa in the OpenEXR format of the HDR image has less impact on the image quality. These schemes mentioned above mainly rely on the characteristics of HDR image formats, and have achieved certain effect in imperceptibility and embedding capacity, but they are powerless in robustness, especially for TMOs. To solve these problems, some other watermarking techniques have been proposed. Guerrini et al. [14] used quantization index modulation (QIM) to design a HDR image detectable watermarking system with the requirements of imperceptibility and robustness against seven kinds of TMOs as well as security. But the bit error rate (BER) in this algorithm is higher than 20%. Xue et al. [15] proposed two HDR image watermarking schemes based on μ -Law and bilateral filtering, respectively. Maiorana et al. [16] proposed a blind multi-bit watermarking scheme based on the properties of the Radon-discrete cosine transform (RDCT) and QIM nonuniform quantizer, however, its BER is also as high as 22%. Solachidis et al. [17] proposed a scheme to embed the multi-bit watermark, based on a perceptual mask obtained with just noticeable difference and contrast sensitivity function. This scheme's shortcoming is the limited capacity of 128 bits. In addition, based on bracketing decomposition, Solachidis et al. [18] also presented another HDR image watermarking scheme, in which a subset of the LDR images is obtained through bracket decomposition, and then the additive spread-spectrum watermarking is applied to wavelet coefficients of each LDR images. But this scheme may result in poor imperceptibility. Wu et al. [19] used a special TMO to process HDR image in advance, and embedded watermark into the obtained LDR image, then reconstructed into watermarked HDR image. This method is robust to some pre-determined TMOs. Obviously, it is not realistic in practical applications. Based on the characteristics of HDR image, the aforementioned algorithms have made some effects on the robustness against TMO attacks from different perspectives. However, the essential distinction between HDR watermarking and LDR watermarking is not

found fundamentally, especially in the effect of TMOs on HDR image watermarking, the analysis is not deep and accurate enough. Therefore, the robustness in the respects of TMOs and the BER still needs to be improved further.

In this paper, a novel robust HDR image watermarking algorithm is proposed, which is not only robust to most TMOs, but also takes into account the imperceptibility and embedded capacity. Firstly, the concept of watermarking activity (WA) is put forward and used, the watermark embedding capacity of the proposed algorithm is improved by the redundant discrete wavelet transform (RDWT). Then, the embedding strength is enhanced by modifying the structure information of HDR image with the singular value decomposition (SVD). Finally, a perceptual brightness mask (PBM) with low complexity is designed to adaptively adjust the imperceptibility of the watermarked image. Experimental analysis shows positive results and demonstrates the effectiveness of designed HDR image watermarking algorithm, compared with the state-of-art algorithms robust against TMOs.

The proposed algorithm has two prominent contributions. On the one hand, it does not rely on HDR image storage format, but directly embed watermark within the raw floating-point number. Therefore, the processes of watermark embedding and extracting are not affected by reading, writing and mutual conversion among the existing RGBE, OpenEXR and LogLuv (TIFF) HDR image formats. On the other hand, through the detailed analysis of the TMOs, we put forward the idea of WA to clarify the essential difference between HDR image watermarking and LDR image watermarking, and successfully propose a highly robust HDR watermarking scheme for TMOs according to this idea.

The remainder of the paper is organized as follows. Related works of HDR and TMO are described in Section 2. Section 3 details the HDR watermark feature and the proposed algorithm. Section 4 shows experimental results and discussion. Finally, summary is given in Section 5.

2. Related Work

This section surveys the related knowledge of HDR image and transformation function. First, a brief description of the HDR image is given, and then the property of TMO is described in detail. Finally, the properties of RDWT and SVD are presented.

2.1 HDR image

Dynamic range in image processing represents the span of the change of a certain physical quantity, that is, the change region between the minimum value and the maximum value. For different cases, the dynamic range has different representation. In the case of digital image, the dynamic range d is the logarithm of the ratio for the maximum to the minimum luminance in a digital image, that is $d = \log_{10}(L_{max}/L_{min})$, where the unit of luminosity is cd/m^2 . The dynamic range of image mainly reflects the richness of the detail that the image can record, and it is an important index to measure the image quality.

There is a very wide range of brightness in the real world scene as shown in Fig. 1, changing from $10^{-3}\text{cd}/\text{m}^2$ to $10^6\text{cd}/\text{m}^2$, as much as 9 or 10 orders in the magnitude. For human visual system (HVS), the human eye can observe dynamic range (instantaneous dynamic range) from 3.0 to 4.2 when the pupil does not enlarge nor shrink, otherwise it will reach 9 [20]. Obviously, this ability of human eye cannot be satisfied by the current image representation methods with 8-bit per color channel. At present, the maximum dynamic range that can be captured by most of camera imaging sensors is not more than 3 orders of magnitude, and the recorded pixel values are stored in 8-bit per color channel. For these two reasons, the overexposure or

underexposure often occur in the generated LDR images, resulting in the loss of important scene information. HDR imaging technologies can be used to overcome the shortcomings of LDR sensor and preserve scene information more completely through accurately capturing the real scene of the relative radiation brightness. Meanwhile, HDR image stores a linear value, that is, the value of each pixel is proportional to the measured physical value of the actual environment. Compared with LDR images, HDR images not only help human to identify the scene, but also have important applications in image processing, computer graphics and other fields.

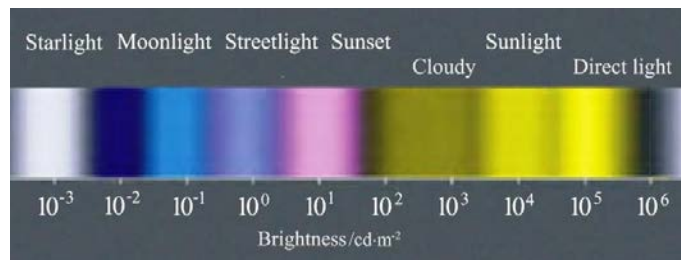


Fig. 1. The brightness range of common light sources [20]

There are many advantages for HDR image, but its data storage is a problem that must be faced. Due to the wide range of brightness, each pixel needs to be stored with floating point data. For HDR image, it means that huge storage space is needed in order to ensure image accuracy. In practical applications, three effective storage formats, including RGBE, OpenEXR and LogLuv (TIFF), are implemented to solve the storage problem. Clearly, the problem of wide brightness range and unique storage format, which are different from LDR images, must be faced for HDR image watermarking.

2.2 Tone Mapping Operator (TMO)

The ultimate goal of HDR image is to present real-world scene brightness to user, but the current general display devices can only show a limited dynamic range of less than three orders of magnitude, which cannot satisfy display of the HDR contents completely. Thus, TMOs are used to reduce dynamic range in HDR images while retaining the maximum perceptible detail information, to adapt the HDR image to the currently conventional displays.

TMOs can be divided into four categories [21], including (1) Global Mapping Algorithm, in which all pixel values in the HDR image are mapped with the same mapping function; (2) Local mapping algorithm, whose parameters can be adjusted in accordance with local information of the HDR image; (3) Segmentation algorithm, in which HDR image is divided into many sub-regions, the pixel values are mapped with different algorithm in different regions; (4) Frequency or gradient domain algorithm, in which the brightness map of HDR image is compressed with multi-scales in the gradient domain, and then it is restored with the new brightness map from the gradient distribution.

TMO adjusts the contrast relationship in HDR image, and the LDR image after mapping retains the details of the scene and the local contrast information, which has achieved good results in reality. However, researchers have made the relevant experiments with TMOs based on psychophysics [22-24], and the test results showed that different TMOs have advantages in different aspects of perception, but no one can achieve the optimal in total aspects. Therefore, the appropriate TMO should be selected to adapt the diverse LDR displays in the actual applications. For HDR image watermarking, it means that the robust algorithm is required to

be valid for all kinds of TMOs. Obviously, this is a great challenge for HDR image watermarking.

2.3 RDWT and SVD property

RDWT is applied in this paper due to its excellent spatial localization, frequency spread, and multi-resolution characteristics which are similar to the theoretical models of the HVS. To describe RDWT, its analysis and synthesis are given in Eq. (1) and Eq. (2), respectively.

$$\begin{cases} c_j[k] = c_{j+1}[k] * h_j[-k] \\ d_j[k] = c_{j+1}[k] * g_j[-k] \end{cases} \quad (1)$$

$$c_{j+1}[k] = \frac{1}{2} (c_j[k] * h_j[k] + d_j[k] * g_j[k]) \quad (2)$$

where $h[-k]$ and $g[-k]$ are the low-pass and high-pass analysis filters and $h[k]$ and $g[k]$ are the corresponding low-pass and high-pass synthesis filters. c_j and d_j are the low-band and high-band output coefficients at level j . The symbol $*$ denotes convolution.

Obviously, RDWT maintains a fixed sampling rate in the decomposition of each level, the redundancy makes it has the spread spectrum characteristic, which can not only increase the watermark embedding information but also enhance the noise immunity of watermarking algorithm.

Currently, various TMOs have now emerged and each TMO has characteristics that differ from those of the others, but the ultimate goal of TM is to generate adaptive LDR data retaining as much information, such as the scene details and the local contrast. Hence, it is suitable to select the perceptible detail information of the HDR image as the watermark carrier. Based on this, the LL-band image obtained by RDWT is used for watermarking in this paper, as it represents the low-frequency information, contains the primary details and can be retained with large probability after TM.

On the other hand, considering SVD from the perspective of linear algebra, a digital image can be regarded as a matrix composed of a number of non-negative scalar terms. Suppose that $I \in R^{N \times N}$ represents such an image matrix, where R represents the real number field, so that I can be expressed as:

$$\begin{aligned} I = USV^T &= [U_1, U_2, \dots, U_N] \begin{bmatrix} \lambda_1 & 0 & 0 & 0 \\ 0 & \lambda_2 & 0 & 0 \\ \vdots & \vdots & \ddots & 0 \\ 0 & 0 & \dots & \lambda_N \end{bmatrix} [V_1, V_2, \dots, V_N]^T \\ &= \lambda_1 U_1 V_1^T + \lambda_2 U_2 V_2^T + \dots + \lambda_N U_N V_N^T \end{aligned} \quad (3)$$

where $U \in R^{N \times N}$ and $V \in R^{N \times N}$ are orthogonal matrixes, whose columns are referred to as singular vectors, and $S \in R^{N \times N}$ is an $N \times N$ diagonal matrix, whose diagonal elements are nonnegative singular values arranged in descending order.

For LDR image, many hybrid image watermarking schemes use SVD with other transforms [25]. Most of them explore the singular values, S , to embed the watermark, due to the limited pixel values in the range of 0 and 255. In addition, embedding the watermark in the U and V components instead of S also has been adopted in a few schemes such as Lai's [26] and Makbol's [27]. In these schemes, the watermark is embedded in the elements of the first column of U matrix. Generally speaking, both U_{21} , U_{31} and U_{31} , U_{41} are suitable to embed the watermark with empirical law. However, when SVD is used in HDR image, some particular

properties, distinguished from LDR image, are presented and would be illustrated in Section 3.2 in detail.

3. The Proposed Robust HDR Image Watermarking Algorithm

The flowchart of the proposed algorithm, including watermark embedding and extraction, is shown in Fig. 2. Firstly, watermarking activity (WA) is defined to clearly specify the regional diversity of robustness in the LDR image after TM. Then, RDWT is used to enhance the robustness for the characteristics of spread spectrum and redundancy. Meanwhile, SVD is adopted to extract the structure information of HDR image and to embed the watermark. Finally, the PBM is defined and extracted to improve the security and reduce the obvious distortion caused by high embedding strength.

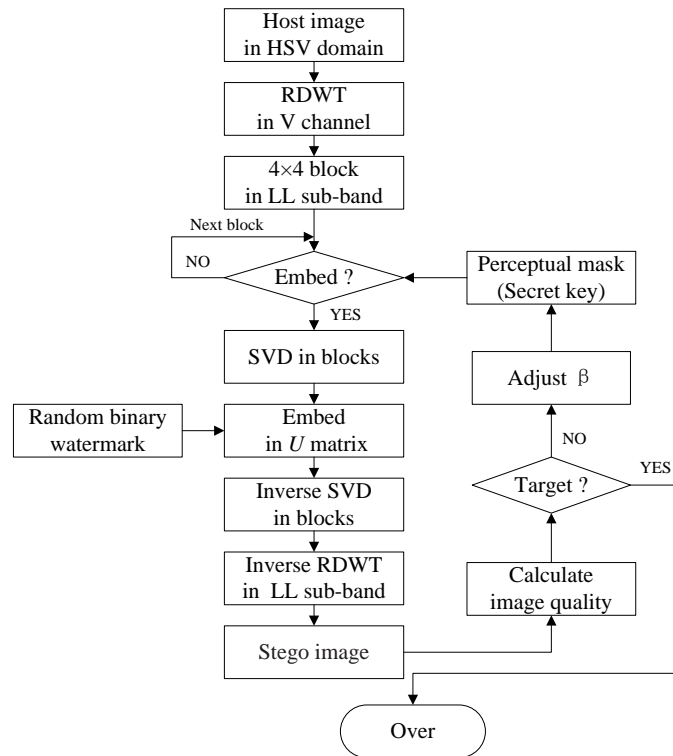


Fig. 2(a). Flowchart of watermark embedding

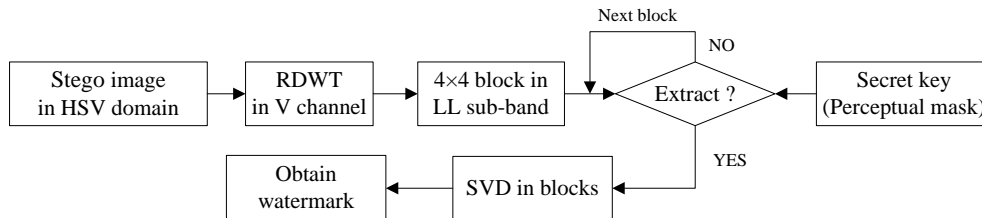


Fig. 2(b). Flowchart of watermark extraction

3.1 Watermarking Activity (WA)

Generally speaking, an image watermarking algorithm consists of design philosophy and embedding intensity. Between them, the former is the core of the algorithm and directly determines the performance of the algorithm, including its imperceptibility, robustness, and other characteristics. The latter is an optimization of the algorithm. Moreover, the image is composed of a series of patches, such as pixels or blocks of different sizes. Therefore, the performance of a watermarking algorithm is also composed of the local performances of these patches in the watermarked image. In other words, when the local performances of these patches are all optimized in some way, the global performance of the image will also be accordingly improved.

Hence, in order to distinguish with the traditional robustness, we put forward the concept of WA to represent the regional diversity of robustness in the watermarked image. More specifically, WA, as a qualitative scalar, indicates the essential robustness of design philosophy. And as the image is composed of a series of patches, the global WA is also composed of a series of local WA for each patch. Obviously, an excellent design philosophy will make the WA the much better, without considering the embedding intensity. Generally speaking, the WA in frequency domain is better than that in spatial domain. Moreover, considering the factor of embedding strength, the final robustness of the algorithm can be expressed as follows:

$$WR = \omega \times WA_G = \omega \times \sum_{k=1}^n \rho(k) WA_L(k) \quad (4)$$

where ω represents the embedding strength, WA_G represents the global watermark activity, n is the region number in the image, $\rho(k)$ denotes the area proportion for the k -th region, $\rho(k) \in [0,1]$ and $\sum_{k=1}^n \rho(k) = 1$, and $WA_L(k)$ denotes the local watermark activity for the k -th region. Eq. (4) shows that the larger the values of ω and WA_G are, the more robust the watermarking algorithm will be. And WA_G can be increased with the improvement of $WA_L(k)$ for each region.

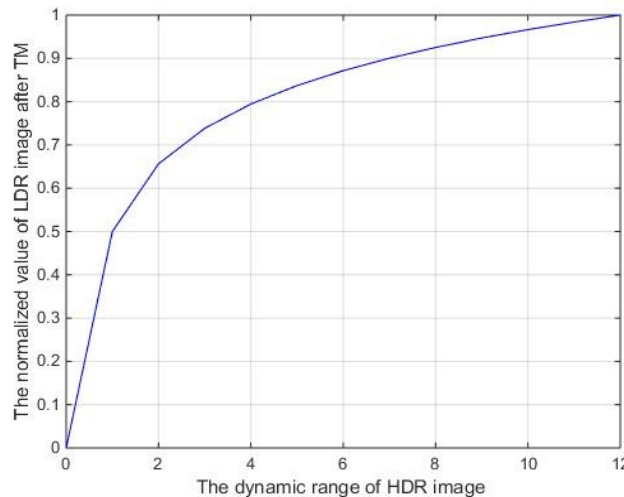


Fig. 3. The schematic diagram of the TMOs

As the WA is determined by its design philosophy, for an LDR image, the varying amplitude of its pixel value is fairly limited when faced with various traditional attacks. Thus, the WA_L for each region are approximately equal to each other, which means that the WA_G

exhibits global equalization characteristics. And because the increase of embedding intensity will reduce the imperceptibility, the trade-off between embedding strength and imperceptibility should be considered. However, for an HDR image, a TM attack can make the pixel values of the different luminance regions fluctuate significantly by more than one order of magnitude, which leads to regional diversity of the WA_L in the tone-mapped images. Meanwhile, the brightness sensitivity of the human eye changes with the variation of the background brightness. The lower the background luminance value is, the higher the sensitivity is, and vice versa. It can be found that as the background brightness increases, the just noticeable difference threshold of the human eye also increases. Based on this, the existing TMOs can be approximately represented as the mapping relationship shown in Fig. 3, where X axis denotes the dynamic range of HDR image, and Y axis denotes the normalized value of LDR image after TM. It is thus clear that, for the HDR image, TMO is a non-linear transformation. The pixel value of LDR image after TM is amplified in low-brightness regions and reduced in high-brightness regions. Thereby, it could achieve the purpose of compressing the dynamic range of brightness. Thus, for the HDR image watermarking, TMO is a non-linear attack. With the enlargement of pixel value in the low-brightness region, the embedded watermark information is amplified too, which means that the LWA of such region is increased or unchanged, and the extraction of the watermark information can be well ensured; otherwise, with the reduction of pixel value in the high-brightness region, the embedded watermark information is lost, which means that the LWA of the region decreases. Hence, if an existing LDR image watermarking algorithm is directly transplanted into the HDR image domain, without taking into account the effect of the LWA, it will result in poor robustness against TMOs, because the LWA in the high-brightness region will decrease after TM.

Generally speaking, once the design philosophy is determined, the WA cannot be changed, thus the robustness can be enhanced only by increasing embedding strength. However, the bigger the embedding strength is, the greater the influence on the quality of the host image is. As a result, the concept of mask can be defined through two ways as follows to improve the robustness of TMOs for HDR watermarking. (1) The robustness can be improved directly by sacrificing imperceptibility and enhancing embedded strength. Afterwards, the imperceptibility could be compensated through the high-distortion mask. (2) The robustness can be enhanced indirectly with the low LWA compensation mask, while reducing embedding strength and improving imperceptibility. Both are the same in nature, which can be weighed according to the complexity of watermarking algorithm and mask algorithm. In this paper, we choose the former to carry on the design of watermarking algorithm and mask algorithm.

3.2 SVD property for HDR image

As discussed in Section 2.3, the original image can be represented as a superimposed sum of the N sub-images after the SVD: $\lambda_1 U_1 V_1^T, \lambda_2 U_2 V_2^T, \dots, \lambda_N U_N V_N^T$. These sub-images are the layers of the original image, and the singular values λ_N , can be regarded as the weight values of brightness for the frame image. Hence, SVD efficiently represents intrinsic algebraic properties of an image, where the diagonal entries of the matrix S specify the luminance of the image, and the corresponding pair of the singular vectors U and V^T specifies the geometry of the image.

According to the research in [28], similar experiments of SVD with 4×4 block in RDWT domain are performed on several HDR images in this paper. The experimental results are shown in Table 1, where the $|U_{i1}|$ denotes the absolute value of the i -th element in the first column in U matrix. And it can be found that all the elements in the first column of U matrix

have the same sign and the values are very close with each other. This peculiarity can be used to embed watermarking.

Here, we choose two elements from U_{11} , U_{21} , U_{31} and U_{41} as the carriers, and embed watermark by modifying the relation between the two elements selected. The specific embedding method will be shown in Eq. (8). The corresponding experimental results are shown in **Table 2**. In the table, PSNR, SNR and VDP_Q denote the values of Peak Signal to Noise Ratio, Signal to Noise Ratio and image quality of HDR-VDP-2 [29] for a watermarked HDR image with respect to its host image, respectively. And BER is the bit error rate. In addition, VDP_Q and BER can be calculated by:

$$VDP_Q = \frac{1}{F \cdot O} \sum_{f=1}^F \sum_{o=1}^O \mathbf{w}_f \log \left(\frac{1}{I} \sum_{i=1}^I \mathbf{D}_p^2[f, o](i) + \varepsilon \right) \quad (5)$$

where i is the pixel index, \mathbf{D}_p denotes the noise normalized difference of the f -th spatial frequency ($f = 1$ to F) band and the o -th orientation ($o = 1$ to O) of the steerable pyramid for the reference and test images, $\varepsilon = 10^{-5}$ is a constant to avoid singularities when \mathbf{D}_p is close to 0, and I is the total number of pixels. \mathbf{w}_f is the vector of per-band pooling weights, which can be determined by maximizing correlations with subjective opinion scores.

$$BER = \frac{N_{error}}{N_{total}} \times 100\% \quad (6)$$

where N_{total} is the number of total bits of the watermark, and N_{error} denotes the number of error bits after watermark extraction.

Table 1. The mean and variance in the first column of U matrix after SVD

Image	$ U_{11} $		$ U_{21} $		$ U_{31} $		$ U_{41} $	
	Mean	Variance	Mean	Variance	Mean	Variance	Mean	Variance
1	0.4967	0.0859	0.4926	0.0617	0.4925	0.0602	0.4960	0.0856
2	0.4987	0.0732	0.4942	0.0433	0.4945	0.0466	0.4981	0.0704
3	0.4960	0.0874	0.4912	0.0567	0.4921	0.0530	0.4989	0.0891
4	0.4989	0.0659	0.4951	0.0383	0.4954	0.0348	0.4991	0.0667
5	0.4961	0.0745	0.4945	0.0441	0.4950	0.0441	0.4990	0.0770
6	0.4970	0.0706	0.4956	0.0441	0.4959	0.0437	0.4976	0.0710
7	0.4990	0.1250	0.4779	0.0996	0.4801	0.0975	0.4910	0.1263
8	0.4949	0.0923	0.4899	0.0645	0.4918	0.0575	0.4985	0.0934
9	0.4932	0.1199	0.4857	0.0775	0.4858	0.0742	0.4947	0.1198
10	0.4982	0.0632	0.4947	0.0454	0.4953	0.0383	0.4999	0.0651
11	0.4985	0.0669	0.4955	0.0445	0.4954	0.0371	0.4982	0.0670
12	0.4984	0.0575	0.4963	0.0373	0.4965	0.0331	0.4997	0.0579
13	0.4967	0.0859	0.4926	0.0617	0.4925	0.0602	0.4960	0.0856
14	0.4982	0.0563	0.4968	0.0330	0.4973	0.0322	0.4992	0.0573
15	0.4986	0.0590	0.4967	0.0328	0.4968	0.0318	0.4988	0.0595
Average	0.4973	0.0789	0.4926	0.0523	0.4931	0.0496	0.4976	0.0795

Table 2. The experimental data of different combinations for the U matrix

	PSNR(dB)	SNR(dB)	VDP_Q	BER(%)
U_{11}, U_{21}	79.4277	30.7536	74.8702	19.32
U_{31}, U_{41}	81.9229	33.2489	77.5468	19.04
U_{11}, U_{31}	79.4022	30.7282	73.9067	12.95
U_{21}, U_{41}	79.3392	30.6651	74.6414	12.59
U_{11}, U_{41}	79.2295	30.5555	73.2207	16.11
U_{21}, U_{31}	81.3498	32.6757	77.4003	19.25

It can be found that the effects of different combinations are slightly different according to image quality and BER. Different from the LDR image as shown in Section 2.3, neither U_{21} , U_{31} nor U_{31} , U_{41} could be used to embed the watermark for HDR image owing to the bad BER of 19%. Therefore, considering the BER and the quality of the watermarked image, both U_{11} , U_{31} and U_{21} , U_{41} are suitable for watermark embedding, and the later is selected in this paper.

3.3 Perceptual brightness mask (PBM)

In HDR image, the use of floating point data results in significant differences in the pixel values compared with LDR image, as much as 9 or 10 orders in the magnitude, between the high brightness and low brightness regions. In this paper, the algorithm embeds watermark by modifying the structure information of HDR image, which causes the variations of pixel values of high brightness region to be much higher than that of the low brightness region. These large changes of pixel values can cause perceived image distortion. Hence, a perceptual brightness mask is defined to improve the imperceptibility of watermark. According to different image quality requirements, the low distortion region can be reserved and the high distortion region can be discarded. Thereby, the size of embedding region can be adjusted adaptively to meet different requirements.

The complexity of the used mask algorithm is very low. First, the HDR image is converted to hue-saturation-value (HSV) format, the V channel is normalized in logarithm, and then the binary processing is performed in accordance with the following Eq. (7).

$$\text{Mask}(\beta) = \begin{cases} 0, & \text{if } L \geq \beta \\ 1, & \text{otherwise} \end{cases} \quad (7)$$

where L indicates the logarithmic normalized value of HDR luminance, β is the weighting coefficient, and $\beta \in [0,1]$, which can be adjusted adaptively to satisfy different quality requirements of the watermarked HDR image.

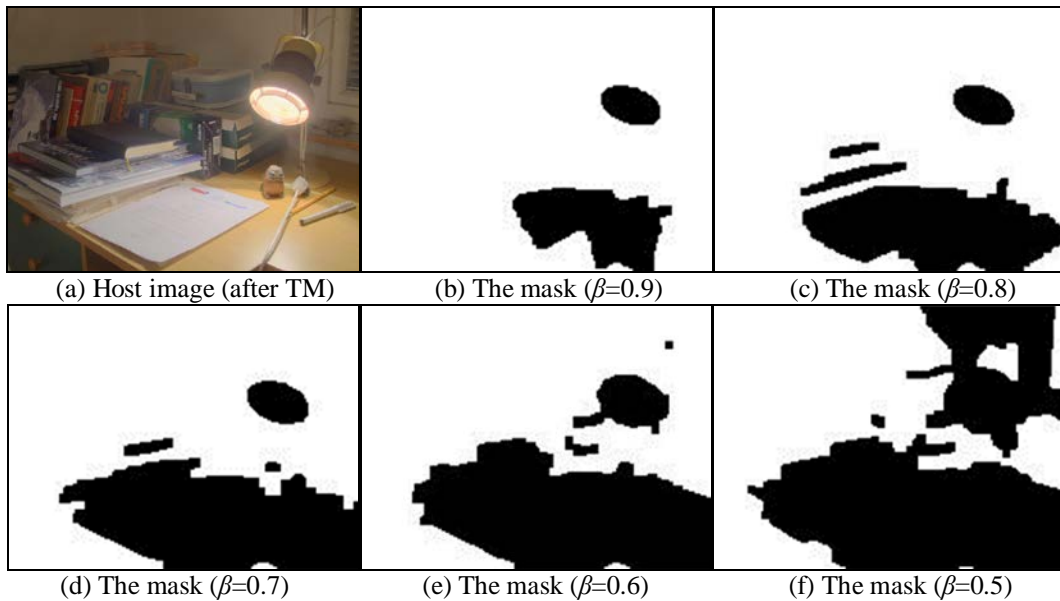


Fig. 4. The host image and the masks with different weighting coefficients

The watermark could be embedded in the regions of $\text{Mask}(\beta)=1$. Here, HDR image named "Light" with the size of 713×535 and the dynamic range of 5.7, which can well reflect the characteristics of HDR images, is chosen as an example. The masks under different weighting coefficients are shown in Fig. 4. It is clear that the mask can effectively segment the image according to the change of the brightness threshold, and meet the requirement of imperceptibility. Simultaneously, the storage space of the mask is small so that the mask can be used as a secret key.

3.4 Watermark embedding and extraction procedures

HDR images with different storage formats are stored with 16-32 bits per color channel in different ways to ensure the image accuracy, but ultimately translated into the same floating-point data to record pixel information. In this paper, we directly embed the watermark information in the floating point data in order to get rid of the shackles of HDR image storage format. In addition, Poulit et al. [30] considered that the original saturation value and chrominance value contained in HDR image can be used to characterize the LDR image after TM, and then the color can be corrected to make the mapped image more realistic. Therefore, it is reasonable to embed the watermark in the luminance domain merely. Here, the first step of the proposed algorithm is to extract luminance component from the HSV color space for watermarking purpose, while chrominance components will be left untouched.

A. Watermark embedding

The watermark embedding procedure is described as follows.

Step 1. Transforming the HDR image into HSV color space.

Step 2. Performing RDWT on V channel of the HDR image, and dividing the LL sub-band into 4×4 non-overlapping blocks.

Step 3. For each 4×4 block, judging whether the block is used to embed watermark or not according to the PBM (Secret key). If it is, turn to Step 4, otherwise the next block will be checked. Note that, the initial value of β is set to 1, meaning that all regions of the HDR image are used to embed the watermark.

Step 4. For a block used to embed watermark, firstly performing SVD on the block. Then watermark is embedded by changing the relation between the U_{21} and U_{41} elements in the first column of U matrix. If w , which is the binary watermark bit to be embedded, is '1', the sign of $(U_{21} - U_{41})$ should be negative and its magnitude is greater than a threshold T ; otherwise, if the w is '0', the value of $(U_{21} - U_{41})$ should be positive and its magnitude is greater than a threshold T . When these two conditions are violated, U_{21} and U_{41} should be modified respectively, based on the following rules in Eq. (8).

$$\begin{aligned} \text{if } w=1 \text{ and } |U_{21} - U_{41}| < T, & \begin{cases} U_{21}^* = \text{sign}(U_{21}) \times (U_{\text{avg}} + T/2) \\ U_{41}^* = \text{sign}(U_{41}) \times (U_{\text{avg}} - T/2) \end{cases} \\ \text{if } w=0 \text{ and } |U_{21} - U_{41}| < T, & \begin{cases} U_{21}^* = \text{sign}(U_{21}) \times (U_{\text{avg}} - T/2) \\ U_{41}^* = \text{sign}(U_{41}) \times (U_{\text{avg}} + T/2) \end{cases} \end{aligned} \quad (8)$$

where $|X|$ denotes the absolute value of X , $\text{sign}(x)$ presents the sign of X and $U_{\text{avg}} = (|U_{21}| + |U_{41}|)/2$. In addition, T is the threshold of embedding intensity, and the larger the value is, the higher the embedding strength is. After the binary watermark bit is embedded in the block, the inverse SVD is performed to obtain the stego block.

Step 5. Repeat Step 3 and Step 4 until all blocks have been processed, and then the stego LL sub-band is reconstructed.

Step 6. Performing the inverse RDWT with the reconstructed LL sub-band to obtain the stego image.

Step 7. According to the calculated HDR-VDP-2 value of the watermarked image, judging whether the preset imperceptibility (the default HDR-VDP-2 value) is reached or not. If the target is reached, the final perceptual mask is set to be the secret key, and the algorithm will be ended. Otherwise, the value of β is reduced by the fixed step length of 0.01 to update the perceptual mask, then repeat Steps 3-7 again until the preset target is reached.

B. Watermark extraction

The proposed algorithm is blind that the watermark extraction only needs the watermarked HDR image or the LDR image after TM. The watermark extraction procedure is described as follows.

Step 1. Transforming the watermarked image into HSV color space.

Step 2. Performing RDWT on V channel of the watermarked image, and dividing the LL sub-band into 4×4 non-overlapping blocks.

Step 3. For each 4×4 block, judging whether the block is embedded watermark or not according to the PBM (Secret key). If it is, turn to Step 4, otherwise the next block will be checked.

Step 4. For a block embedded watermark, performing SVD on the block. Then the watermark is extracted according to the relation between U_{21}^* and U_{41}^* in the first column of the U matrix:

$$w^* = \begin{cases} 0, & \text{if } U_{21}^* > U_{41}^* \\ 1, & \text{otherwise} \end{cases} \quad (9)$$

Step 5. Repeat Step 3 and Step 4 until all blocks have been processed. Then the watermark can be obtained by arranging the extracted binary values.

4. Experimental results and discussion

In order to verify the effectiveness of the proposed HDR image watermarking algorithm, we implement our scheme in Matlab2014b platform, with the public HDR image library and the existing TMOs collected from two sources. (1) The source of the HDR image library. The HDR image database used in our experiments is a heterogeneous set of 32-bit encoded images collected from two sources: The Greg Ward's website repositories [31], including 33 images with dynamic range from 2.0 to 8.9 and size from 512×346 to 6144×6144 ; The Image Gallery's website repositories [32], including 7 images with dynamic range from 3.0 to 8.6 and size from 760×1016 to 3270×1396 . (2) The source of the TMO. The Banterle's HDR Toolbox for Matlab [5], including 27 TMOs, and vision is 1.1.0.

In this paper, 30 images are used to test the watermarking schemes, including 15 large images and 15 small images, and 26 TMOs are used as TM attacks. The selection was performed so as to provide some variety in terms of subjects being represented as well as image sizes and dynamic ranges. Table 3 reports the images with the relevant data. The TMOs considered are those available by the library, as shown in Table 4.

For LDR image, the PSNR, Structural Similarity (SSIM) are recognized as the evaluation benchmark, but the 8-bit per color channel cannot meet the storage requirements for HDR image, as its dynamic range is up to 9. Generally speaking, the 32-bit per color channel is

chosen to ensure image accuracy in the formats of RGBE, OpenEXR, LogLuv (TIFF). Thus, the objective quality of the HDR image can be characterized more accurately by SNR than by PSNR as demonstrated by Hanhart et al. [33]. Moreover, Hanhart et al. conducted a comprehensive comparison of image quality evaluation with various algorithms and found that HDR-VDP-2 has the most objective quality evaluation of HDR images in linear space, as Pearson linear correlation coefficient and Spearman rank correlation coefficient are 0.9604 and 0.9564. Thus, the SNR, SSIM and HDR-VDP-2 are used to evaluate the imperceptibility of the algorithm, and the BER is used to measure the robustness of the algorithm.

Table 3. List of the used HDR images in the test database

Image No.	Image Name	Image Size	Source	Image No.	Image Name	Image Size	Source
1	Apartment	2048×1536	[31]	16	rend06	1024×1024	[31]
2	AtriumNight	760×1016	[31,32]	17	rend07	575×575	[31]
3	bigFogMap	751×1130	[31]	18	rend10	1024×1024	[31]
4	dani_belgium	1025×769	[31]	19	rend13	1024×1024	[31]
5	dani_cathedral	767×1023	[31]	20	rosette	720×480	[31]
6	dani_synagogue	1025×769	[31]	21	Spheron3	2149×1074	[31]
7	Desk	644×874	[31]	22	SpheronNice	2981×1165	[31]
8	Display1000	2048×1536	[31]	23	SpheronSiggraph	1329×1289	[31]
9	memorial	512×768	[31]	24	StillLife	1240×846	[31]
10	Montreal	2048×1536	[31]	25	Tree	928×906	[31]
11	MtTamWest	1214×732	[31]	26	AtriumMorning	760×1016	[32]
12	nave	720×480	[31]	27	mpi_atrium	1024×676	[32]
13	rend01	1024×1024	[31]	28	nancy_cathedral_1	1536×2048	[32]
14	rend02	1000×676	[31]	29	nancy_cathedral_2	1536×2048	[32]
15	rend03	1000×676	[31]	30	snow	2048×1536	[32]

Table 4. List of the used 26 Tone Mapping Operators

TMO No.	TMO Name	Time	TMO No.	TMO Name	Time
1	Ashikhmin	2002	14	Logarithmic	
2	BruceExpoBlend	2013	15	Mertens	2007
3	Chiu	1993	16	Normalize	
4	Drago	2003	17	Pattanaik	2000
5	Durand	2002	18	RamanTMO	2009
6	Exponential		19	ReinhardDevlin	2005
7	Fattal	2002	20	Reinhard	2002
8	Ferwerda	1996	21	Schlick	1995
9	Gamma		22	TumblinRushmeier	1993
10	KimKautzConsistent	2008	23	VanHateren	2006
11	Krawczyk	2005	24	WardGlobal	1994
12	Kuang	2007	25	WardHistAdj	1997
13	Lischinski	2006	26	Yee	2003

4.1 Parameter setting

According to the watermark embedding process in Section 3, the value of T determines the embedding intensity. Obviously, the quality influence with various T values is also different, as shown in **Table 5**. In the table, SNR and VDP_Q denote the image quality of watermarked HDR image, BER1 is the extraction error rate of the watermarked HDR image, and BER2 is the extraction error rate of the watermarked LDR image after TM. With the increase of T value, the HDR image quality (SNR and VDP_Q) and watermarking error rate (BER1 and BER2) show a downward trend. This is more intuitive in **Fig. 5**. It is clear that the degradation rate of image quality and bit error rate is slow down when $T=0.04$ and $T=0.08$. Here we select $T=0.08$ for the trade-off, which can ensure a relative low BER, while the image quality of the watermarked HDR image is also in an accepted range, and it can be improved after using the PBM.

Table 5. The quality influence with various T values

T	SNR(dB)	VDP_Q	BER1(%)	BER2(%)
0.01	53.1260	93.1239	35.40	37.68
0.02	45.7346	86.4864	26.59	29.33
0.04	37.6736	80.0894	19.20	21.40
0.08	30.8063	74.7812	12.50	14.05
0.12	26.5798	71.1860	9.25	10.86
0.16	23.2793	68.4244	7.05	7.98

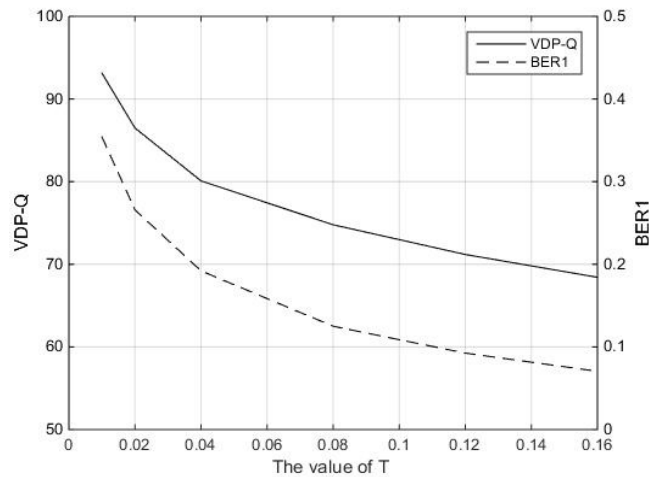


Fig. 5. The curves of VDP_Q and BER following T values in the proposed algorithm.

4.2 PBM evaluation

In order to improve the imperceptibility of the proposed algorithm further, an adaptive PBM is designed in Section 3, which can automatically adjust the size of the embedding region according to different image quality requirements. Here, the HDR image named "Light" is

chosen as an example, and the marking process is performed on the embedding region with the embedding intensity $T=0.08$. As shown in **Table 6**, with the decrease of the value of β , the high-distortion region of the HDR image is reduced, so the image quality (imperceptibility) is improved, while the BER is almost unchanged. In this paper, the value of β is automatically adjusted with default value HDR-VDP-2=90, and the concrete data is shown in Section 4.4. The results show that, after using the PBM, the β value can be automatically adjusted to achieve the desired target according to the pre-set image quality (imperceptibility), thus the flexible imperceptibility and embedded capacity can be achieved.

Table 6. The image quality of the watermarked HDR image "Light" and BER with various β values

SNR(dB)	VDP_Q	SSIM	Capacity(bit)	BER(%)	β
30.9461	74.6456	1.0000	23986	12.74	1.00
54.5889	85.0219	1.0000	21321	12.42	0.90
61.9572	89.9308	1.0000	18714	12.61	0.80
67.4547	94.4129	1.0000	17078	11.21	0.70
69.6194	96.0589	1.0000	15855	10.75	0.60
73.9109	98.3092	1.0000	12346	11.31	0.50

4.3 Robustness against traditional attacks

To evaluate the robustness of the watermarking algorithm against conventional attacks, a random binary watermark is embedded into the HDR host images in **Table 3**, and the results of BER obtained from the watermarked HDR image are given in **Table 7**, which shows that the robustness is already satisfactory.

Table 7. The BER of the watermarked HDR image with various conventional attacks

Attack		BER(%)	Attack		BER(%)
NO attack		9.96	Median filter		17.26
Noise addition	Poisson	10.32	Affine		13.54
	Pepper salt	23.05	Crop	1/4	20.33
Rotation	5°	12.27		1/9	14.48
	15°	15.52		1/16	12.86
	30°	19.43		1/25	11.21
	45°	20.78	Scaling	2	10.59
90°	19.65	1/2		17.38	

4.4 Robustness against TMOs

To evaluate the robustness against the TMOs and the imperceptibility of the proposed algorithm, a random binary watermark is embedded into the host HDR images. The results of the BER with respect to large as well as small LDR watermarked images obtained with different TMOs are shown in **Fig. 6**. The average results are given in **Table 8**, with the value less than 12.42%. Clearly, the robustness against TMO is excellent.

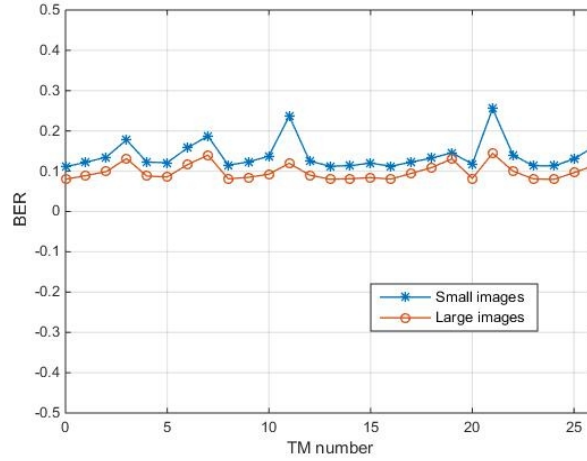


Fig. 6. The BER with different TMOs for large images and small images

Table 8. The results of the BER with different TMOs

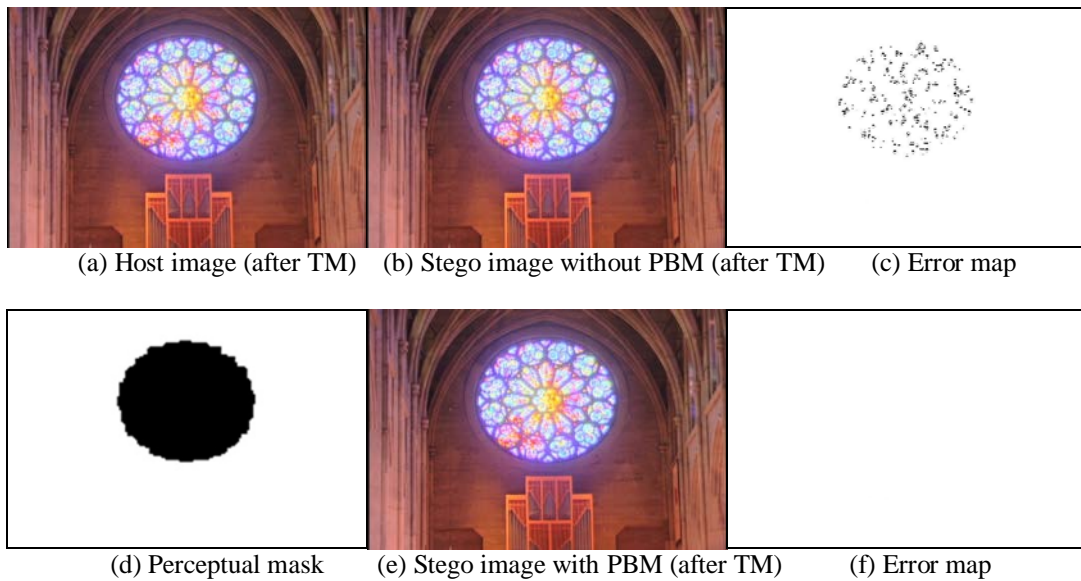
TMO No.	BER(%)	TMO No.	BER(%)	TMO No.	BER(%)	TMO No.	BER(%)
NO TM	9.96	7	16.72	14	10.11	21	20.46
1	10.73	8	10.62	15	10.83	22	12.31
2	12.05	9	10.87	16	10.23	23	10.11
3	15.73	10	12.17	17	11.35	24	9.35
4	10.82	11	18.56	18	12.74	25	11.64
5	10.58	12	11.51	19	14.23	26	13.24
6	14.14	13	10.65	20	10.39	Average	12.42

Table 9. The results without PBM ($T=0.08$)

Image No.	SNR (dB)	VDP_Q	Capacity (bit)	BER (%)	β	Image No.	SNR (dB)	VDP_Q	Capacity (bit)	BER (%)	β
1	28.05	66.03	196608	9.22	1.00	16	29.37	71.89	65536	5.24	1.00
2	29.15	74.21	48260	9.57	1.00	17	30.60	77.63	20736	12.25	1.00
3	31.09	72.59	53204	12.00	1.00	18	68.72	99.50	65536	8.24	1.00
4	28.99	71.49	49601	12.93	1.00	19	30.64	70.51	65536	3.85	1.00
5	30.09	69.48	49152	11.00	1.00	20	36.05	81.55	21600	14.14	1.00
6	28.04	61.87	49601	10.39	1.00	21	70.59	99.65	144722	7.04	1.00
7	29.05	73.50	35259	7.18	1.00	22	30.30	83.46	217832	9.81	1.00
8	33.79	74.15	196608	9.81	1.00	23	30.41	72.45	107559	4.76	1.00
9	35.47	80.38	24576	13.38	1.00	24	28.43	82.15	65720	12.17	1.00
10	33.83	78.17	196608	7.87	1.00	25	28.50	66.76	52664	14.95	1.00
11	27.97	64.57	55632	11.49	1.00	26	29.81	74.17	48260	9.48	1.00
12	36.72	86.92	21600	9.76	1.00	27	31.71	79.92	43264	12.30	1.00
13	28.32	74.75	65536	9.12	1.00	28	33.13	81.62	196608	8.38	1.00
14	32.68	75.49	42250	10.61	1.00	29	31.68	79.49	196608	9.08	1.00
15	31.50	72.96	42250	7.09	1.00	30	28.13	68.67	196608	15.80	1.00

Table 10. The results with PBM when HDR-VDP-2=90 ($T=0.08$)

Image No.	SNR (dB)	VDP_Q	Capacity (bit)	BER (%)	β	Image No.	SNR (dB)	VDP_Q	Capacity (bit)	BER (%)	β
1	71.25	83.79	61355	10.99	0.31	16	56.01	84.54	11626	7.30	0.18
2	65.44	89.06	13714	12.61	0.28	17	34.09	84.03	12912	13.86	0.62
3	57.85	90.75	25665	9.15	0.48	18	68.72	99.50	65536	8.24	1.00
4	60.89	88.05	19898	13.76	0.40	19	45.82	87.02	13860	8.10	0.21
5	72.22	87.96	16673	11.70	0.34	20	68.92	89.05	18175	9.91	0.84
6	51.16	88.01	13207	10.53	0.27	21	70.59	99.65	144722	7.04	1.00
7	86.20	90.54	11157	5.81	0.32	22	32.60	90.75	112991	18.20	0.52
8	79.95	91.79	16323	9.43	0.08	23	69.08	89.02	67491	5.10	0.63
9	67.78	89.53	15591	12.76	0.63	24	52.28	89.43	59251	10.09	0.90
10	57.50	89.84	114101	9.44	0.58	25	90.12	90.71	13144	12.56	0.26
11	74.58	86.76	20158	10.40	0.36	26	61.79	89.20	19741	10.70	0.41
12	73.68	95.55	20786	9.24	0.96	27	57.67	88.83	17812	8.31	0.41
13	29.29	90.22	22407	2.58	0.34	28	66.94	89.15	166167	7.32	0.85
14	55.07	87.97	35295	13.19	0.84	29	66.20	88.36	151221	7.90	0.77
15	47.59	89.19	12227	7.43	0.29	30	61.82	85.17	32433	10.87	0.16

**Fig. 7.** The related images and error maps of the test with PBM for image 20 (small)

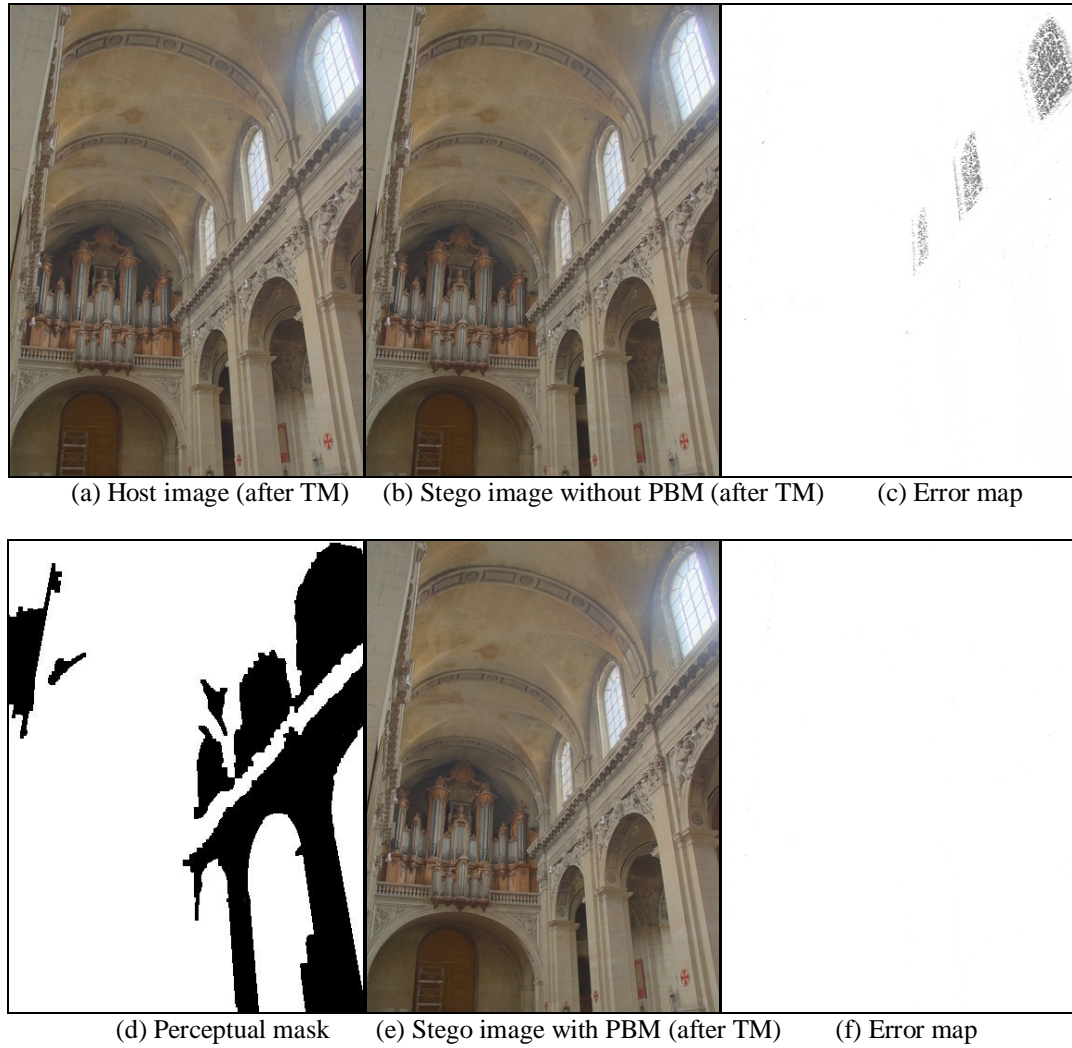


Fig. 8. The related images and error maps of the test with PBM for image 29 (large)

The effect of the PBM are given in [Table 9](#) and [Table 10](#). [Figs. 7](#) and [8](#) also show the Stego image obtained without or with the PBM in which image 20 and image 29 are used as the test images, in the experiments, the HDR-VDP-2 value is set to a default value 90. [Table 9](#) presents that the quality of the watermarked image is different due to the difference of texture detail, dynamic range and contrast for different HDR images, but the VDP-Q values are still more than 60 when $T=0.08$, which facilitates PBM to improve the imperceptibility further. [Table 10](#), [Figs. 7](#) and [8](#) illustrate that, after using the PBM, the average value of the BER changes a little but the imperceptibility of the image is further improved, and the embedded capacity keeps above 10^4 bit and 10^5 bit for small image and large image respectively, which is an excellent result for watermarking.

4.5 Comparison with the state-of-art algorithms

We compared the performance of the proposed algorithm with some of the state-of-art algorithms including the Guerrini's algorithm based on discrete wavelet transform (DWT) [14], Maiorana's algorithm based on DWT-RDCT [16] and Wu's algorithm based on discrete cosine transform (DCT) [19] in the terms of robustness against TMO, embedding capacity and imperceptibility. For the sake of fairness, we chose the same test images and TMOs in [14] and [16], respectively. The comparison results are shown in Table 11, Table 12 and Table 13. In view of the fact that TMO needs to be pre-determined in literature [19], which is lack of practicality, we did not compare the proposed algorithm with the Wu's algorithm in detail.

Table 11. The comparison with Guerrini's algorithm [14] in capacity and BER with TMO

Image	Algorithm	Capacity (bit)	BER (%)					
			NO TM	TM4	TM5	TM7	TM17	TM19
2	Guerrini's	666	15.32	19.52	30.63	38.44	27.33	21.32
	Proposed	13714	12.61	12.82	13.13	20.26	13.46	14.19
3	Guerrini's	737	13.70	17.23	27.54	37.86	23.47	16.01
	Proposed	25665	9.15	9.04	9.36	15.12	10.56	10.72
4	Guerrini's	666	26.28	30.18	33.63	39.49	31.83	33.48
	Proposed	19898	13.76	14.29	16.12	23.15	16.19	14.19
10	Guerrini's	3106	28.40	30.14	29.97	35.61	32.49	32.20
	Proposed	114101	9.44	11.25	10.37	18.89	11.98	19.12
13	Guerrini's	938	24.63	26.12	35.39	36.35	28.68	27.40
	Proposed	22407	2.58	2.71	2.66	4.08	3.09	2.89

Table 12. The comparison with Maiorana's algorithm [16] in capacity and BER with TMO

Image	Algorithm	Capacity (bit)	BER (%)					
			NO TM	TM4	TM5	TM12	TM19	TM22
12	Maiorana's	882	29.12	33.88	36.58	36.26	33.08	33.99
	Proposed	20786	9.24	10.75	10.26	9.96	15.47	21.22
17	Maiorana's	768	22.26	30.73	25.91	33.98	28.39	30.08
	Proposed	12912	13.86	14.41	14.96	14.97	14.99	15.29
18	Maiorana's	2700	22.22	30.44	27.70	32.81	24.19	30.22
	Proposed	65536	8.24	9.10	9.47	10.76	9.54	11.33
26	Maiorana's	1914	0.16	6.95	23.77	14.84	7.21	23.98
	Proposed	19741	10.70	10.81	11.47	12.25	12.52	10.98
28	Maiorana's	8100	6.69	25.26	15.33	31.26	18.68	19.38
	Proposed	166167	7.32	8.16	7.70	8.27	22.66	9.75

Table 13. The comparison of comprehensive performance

Term		Guerrini's [14]	Maiorana's [16]	Wu's [19]	Proposed
Number of test image		15	7	4	30
Number of test TMO		7	6	4	26
Average of BER(%)	No TM	21.73	6.09	30.05	9.96
	TM	29.82	19.25	30.44	12.42
HDR-VDP-2	VDP_Q	76-95	70-93	65-89	84-100
	VDP_95 (%)	0.22	1.96	2.53	0
	VDP_75 (%)	0.46	3.65	5.76	0.04
Capacity (bit)		298-3106	768-8100	4800	10^4 - 10^5

Table 11 shows that Guerrini's algorithm, which is with the complex perceptual mask based on luminance, activity and edge terms, sacrifices the capacity to favor the requirement of imperceptibility. **Table 12** illustrates that for Maiorana's algorithm, which embedding the watermark in HH sub-band in DWT domain, the capacity dropped dramatically to meet the requirement of imperceptibility. In this paper, we design a low-complexity PBM based on the brightness. When setting VDP-Q=90 as default, the embedding capacity is more than 20 times of that in [14] and [16]. Meanwhile, the BER of the proposed algorithm, no matter with or without TMO, are obviously better than that of the algorithms in [14] and [16]. In summary, the proposed algorithm based on RDWT-SVD is superior to the DWT, DWT-RDCT and DCT transforms based algorithms in the terms of number of test image and TMO, robustness, imperceptibility, and capacity as shown in **Table 13**. And in this table, as a full-reference visual difference metric, on the one hand, the output (VDP_Q) of the HDR-VDP-2 denotes the image quality. On the other hand, the output (VDP_95 and VDP_75) of the HDR-VDP-2 is the percentage of pixels that, according to its model, a human observer would perceive as different with a given probability (respectively, 95% and 75%). Hence, larger values of VDP_Q lead to better image quality. Similarly, larger values of VDP_95 (or VDP_75) lead to worse image quality. Obviously, the proposed algorithm shows excellent performance and universal usability.

5. Conclusion

As an important development and breakthrough in digital image, the applications of high dynamic range (HDR) image are more and more extensive. However, the watermarking technology has not kept pace with the rapid development of HDR images, it is powerless especially in the face of the special requirements of tone mapping operators (TMOs). In this paper, through the detailed analysis of the TMOs, we put forward the concept of watermarking activity (WA) to clarify the essential difference between HDR image watermarking and low dynamic range (LDR) image watermarking, and then a robust HDR image watermarking algorithm is proposed against TMO based on redundant discrete wavelet transform and singular value decomposition hybrid transformation. The algorithm embeds the watermark by modifying the structure information of the HDR image, and further enhances the imperceptibility of the watermark through the perceptual brightness mask (PBM). Experimental analysis shows positive results and demonstrates the system effectiveness against current state-of-art TM algorithms.

Although the proposed algorithm is robust to TMOs, further improvements are still possible. For instance, the complexity of PBM is extremely low, but its segmentation accuracy is not satisfactory for natural scene with more texture details. In addition, the bit error rate of the proposed watermarking algorithm are still high for partial TMOs. Thus, future work will focus on further increasing the mask accuracy and reducing the bit error rate for all TMOs.

References

- [1] R. K. Mantiuk, K. Myszkowski and H. P. Seidel, "High dynamic range imaging," *Wiley Encyclopedia of Electrical and Electronics Engineering*, New York, 2016.
[Article \(CrossRef Link\)](#)
- [2] F. Dufaux, P. Le Callet, R. Mantiuk and M. Mrak, "High dynamic range video: from acquisition to display and applications," *1st Edition, Academic Press, Salt Lake City*, 2016.
[Article \(CrossRef Link\)](#)

- [3] Y. Li, C. Lee and V. Monga, "A maximum a posteriori estimation framework for robust high dynamic range video synthesis," *IEEE Transactions on Image Processing*, vol.26, no.3, pp. 1143-1157, March, 2017. [Article \(CrossRef Link\)](#)
- [4] P. Sen and C. Aguerrebere. "Practical high dynamic range imaging of everyday scenes: photographing the world as we see it with our own eyes," *IEEE Signal Process Magazine*, vol.33, no.5, pp. 36-44, September, 2016. [Article \(CrossRef Link\)](#)
- [5] F. Banterle, HDR Toolbox for Matlab, Version: 1.1.0 [Online]. Available: [Article \(CrossRef Link\)](#), 2016.
- [6] P. Campisi, E. Maiorana, K. Debattista and A. Chalmers, "High dynamic range media watermarking issues and challenges," in *Proc. of EUSIPCO 2013 : European Signal Processing Conference*, pp. 1-5, September 9-13, 2013. [Article \(CrossRef Link\)](#)
- [7] C. Yu, K. Wu and C. Wang, "A distortion-free data hiding scheme for high dynamic range images," *Displays*, vol.32, no.5, pp. 225-236, February, 2011. [Article \(CrossRef Link\)](#)
- [8] Z. Wang, C. Chang, T. Lin and C. Lin, "A novel distortion-free data hiding scheme for high dynamic range images," in *Proc. of International Conference on Digital Home*, pp. 33-38, November 23-25, 2012. [Article \(CrossRef Link\)](#)
- [9] C. Chang, T. S. Nguyen and C. Lin, "Distortion-free data embedding scheme for high dynamic range images," *Journal of Electronic Science and Technology of China*, vol.11, no.1, pp. 20-26, August, 2013. [Article \(CrossRef Link\)](#)
- [10] C. Chang, T. S. Nguyen and C. Lin, "A new distortion-free data embedding scheme for high-dynamic range images," *Multimedia Tools and Applications*, vol. 75, no.1, pp. 145-163, January, 2016. [Article \(CrossRef Link\)](#)
- [11] Y. Cheng and C. Wang, "A novel approach to steganography in high dynamic range images," *IEEE Multimedia*, vol.16, no.3, pp. 70-80, September, 2009. [Article \(CrossRef Link\)](#)
- [12] M. Li, N. Huang and C. Wang, "A data hiding scheme for HDR images," *International Journal of Innovative Computing Information and Control*, vol.7, no.5(A), pp. 2021-2035, May, 2011. [Article \(CrossRef Link\)](#)
- [13] Y. Lin, C. Wang, W. Chen, F. Lin and W. Lin, "A novel data hiding algorithm for high dynamic range images," *IEEE Transactions on Multimedia*, vol.19, no.1, pp. 196-211, January, 2017. [Article \(CrossRef Link\)](#)
- [14] F. Guerrini, M. Okuda, N. Adami and R. Leonardi, "High dynamic range image watermarking robust against tone-mapping operators," *IEEE Transactions Information Forensics and Security*, vol.6, no.2, pp. 283-295, June, 2011. [Article \(CrossRef Link\)](#)
- [15] X. Xue, T. Jinno, X. Jin, M. Okuda and S. Goto, "Watermarking for HDR image robust to tone mapping," *IEICE Transactions on Fundamentals of Electronics Communications and Computer Sciences*, vol.94-A, no.11, pp. 2334-2341, November, 2011. [Article \(CrossRef Link\)](#)
- [16] E. Maiorana, V. Solachidis, P. Campisi and Y. Lou, "Robust multi-bit watermarking for HDR images in the Radon-DCT domain," in *Proc. of International Symposium on Image and Signal Processing and Analysis*, pp. 284-289, September 4-6, 2013. [Article \(CrossRef Link\)](#)
- [17] V. Solachidis, E. Maiorana and P. Campisi, "HDR image multi-bit watermarking using bilateral-filtering-based masking," in *Proc. of SPIE 8655, Image Processing: Algorithms and Systems XI*, February 19, 2013. [Article \(CrossRef Link\)](#)
- [18] V. Solachidis, E. Maiorana, P. Campisi and F. Banterle, "HDR image watermarking based on bracketing decomposition," in *Proc. of International Conference on Digital Signal Processing*, pp. 1-6, July 1-3, 2013. [Article \(CrossRef Link\)](#)
- [19] J. Wu, "Robust watermarking framework for high dynamic range images against tone-mapping attacks," *In book: Watermarking, InTech*, vol. 2, pp. 229-242, May, 2012. [Article \(CrossRef Link\)](#)
- [20] E. Reinhard, W. Heidrich, P. Debevec, S. Pattanaik, G. Ward and K. Myszkowski, "High dynamic range imaging: acquisition, display and image-based lighting," *2nd Edition, Academic Press 2010*, Salt Lake City, 2010. [Article \(CrossRef Link\)](#)
- [21] F. Banterle, A. Artusi, K. Debattista and A. Chalmers, "Advanced high dynamic range imaging: theory and practice," *Natick: CRC Press, Boca Raton*, 2011. [Article \(CrossRef Link\)](#)

- [22] A.O. Akyuz, R. Fleming, B.E. Riecke, E.Reinhard and H.H. Bülthoff, “Do HDR displays support LDR content ?: a psychophysical evaluation,” *ACM Transactions on Graphics*, vol.26, no.3, article no.38, July, 2007. [Article \(CrossRef Link\)](#)
- [23] P. Ledda, A. Chalmers, T. Troscianko and H. Seetzen, “Evaluation of tone mapping operators using a high dynamic range display,” *ACM Transactions on Graphics*, vol.24, no.3, pp. 640-648, July, 2005. [Article \(CrossRef Link\)](#)
- [24] M. Cakik, M. Wimmer, L. Neumann and A. Artusi, “Evaluation of HDR tone mapping methods using essential perceptual attributes,” *Computers & Graphics*, vol.32, no.3, pp. 330-349, June, 2008. [Article \(CrossRef Link\)](#)
- [25] Y. Zhang, C. Wang, X. Wang and M. Wang, “Feature-Based Image Watermarking Algorithm Using SVD and APBT for Copyright Protection,” *Future Internet*, vol.9, no.2, article no.13, April, 2017. [Article \(CrossRef Link\)](#)
- [26] C.C Lai, “An improved SVD-based watermarking scheme using human visual characteristics,” *Optics Communications*, vol. 284, no. 4, pp. 938–944, February, 2011. [Article \(CrossRef Link\)](#)
- [27] N. M. Makbol, B. E. Khoo1 and T. H. Rassem, “Block-based discrete wavelet transform-singular value decomposition image watermarking scheme using human visual system characteristics,” *IET Image Process*, vol. 10, no.1, pp. 34–52, January, 2016. [Article \(CrossRef Link\)](#)
- [28] Q. Su, Y. Niu, Y. Zhao, S. Pang and X. Liu, “A dual color images watermarking scheme based on the optimized compensation of singular value decomposition,” *AEU-International Journal of Electronics and Communications*, vol.67, pp. 652-664, August, 2013. [Article \(CrossRef Link\)](#)
- [29] M. Narwaria, R.K. Mantiuk, M.P.D. Silva and P.L. Callet. “HDR-VDP-2.2: a calibrated method for objective quality prediction of high dynamic range and standard images,” *Journal of Electronic Imaging*, vol.24, no.1, article no.010501, January, 2015. [Article \(CrossRef Link\)](#)
- [30] T. Pouli, A. Artusi, F. Banterle, H. Seidel and E. Reinhard, “Color correction for tone reproduction,” in *Proc. of 21st Color and Imaging Conference*, pp. 215-220, November 4-8, 2013.
- [31] Anywhere Software Database [Online]. Available: [Article \(CrossRef Link\)](#).
- [32] Image Gallery [Online]. Available: [Article \(CrossRef Link\)](#).
- [33] P. Hanhart, M.V. Bernardo, M. Pereira, A. M. G. Pinheiro and T. Ebrahimi, “Benchmarking of objective quality metrics for HDR image quality assessment,” *EURASIP Journal on Image and Video Processing*, vol.2015, article no.39, December, 2015. [Article \(CrossRef Link\)](#)



Yongqiang Bai received his B.S. and M.S. degrees from ZhengZhou University, China, in 2006 and 2009 respectively, and he is currently a Ph.D. candidate of Ningbo University, China. His research interests mainly include data hiding, digital watermarking and image processing.



Gangyi Jiang received his M.S. degree from Hangzhou University, China, in 1992, and received his Ph.D. degree from Ajou University, Korea, in 2000. He is now a professor at Faculty of Information Science and Engineering, Ningbo University, China. His research interests mainly include digital video compression and communications, multi-view video coding and image processing.



Hao Jiang received his M.S. degree from Ningbo University, China, in 2008. He is now a researcher in Intelligent Household Appliances Engineering Center, Zhejiang Business Technology Institute, China. His research interests include low complexity video processing and VR technique research.



Mei Yu received her B.S. and M.S. degrees from Hangzhou Institute of Electronics Engineering, China, in 1990 and 1993, and Ph.D. degree from Ajou University, Korea, in 2000. She is now a professor at the Faculty of Information Science and Engineering, Ningbo University, China. Her research interests include image/video coding and video perception



Fen Chen received her B.S. degree from Sichuan Normal College, China, in 1996, and M.S. degree from the Institute of Optics and Electronics, Chinese Academy of Science in 1999, and Ph.D degree from Ningbo University in 2016. She is now an associate professor at the Faculty of Information Science and Engineering, Ningbo University, China. Her research interests mainly include digital signal processing, image processing and communications, and multiview video processing.



Zhongjie Zhu received the Ph.D degree in electronics science and technology from Zhejiang University, China, in 2004. He is currently a professor with Faculty of Electronics and Information Engineering, Zhejiang Wanli University, China. His research interests mainly include video compression and communication, image analysis and understanding, watermarking and information hiding, and 3D image signal processing.